JCI insight

RESEARCH ARTICLE

Proteomics analysis reveals a Th17-prone cell population in presymptomatic graft-versus-host disease

Wei Li,[1] Liangyi Liu,[1] Aurelie Gomez,[2] Jilu Zhang,[1] Abdulraouf Ramadan,[1] Qing Zhang,[3] Sung W. Choi,[2] Peng Zhang,[2] Joel K. Greenson,[2] Chen Liu,[4] Di Jiang,[5] Elizabeth Virts,[1] Stephanie L. Kelich,[1] Hong Wei Chu,[5] Ryan Flynn,[6] Bruce R. Blazar,[6] Helmut Hanenberg,[1] Samir Hanash,[7] and Sophie Paczesny[1]

[1]Indiana University School of Medicine, Indianapolis, Indiana, USA. [2]University of Michigan, Ann Arbor, Michigan, USA. [3]Fred Hutchinson Cancer Research Center, Seattle, Washington, USA. [4]Rutgers-Robert Wood Johnson Medical School, New Brunswick, New Jersey, USA. [5]National Jewish Health, Denver, Colorado, USA. [6]University of Minnesota, Minneapolis, Minnesota, USA. [7]MD Anderson Cancer Center, Houston, Texas, USA.

Gastrointestinal graft-versus-host-disease (GI-GVHD) is a life-threatening complication occurring after allogeneic hematopoietic cell transplantation (HCT), and a blood biomarker that permits stratification of HCT patients according to their risk of developing GI-GVHD would greatly aid treatment planning. Through in-depth, large-scale proteomic profiling of presymptomatic samples, we identified a T cell population expressing both CD146, a cell adhesion molecule, and CCR5, a chemokine receptor that is upregulated as early as 14 days after transplantation in patients who develop GI-GVHD. The $CD4^+CD146^+CCR5^+$ T cell population is Th17 prone and increased by ICOS stimulation. shRNA knockdown of CD146 in T cells reduced their transmigration through endothelial cells, and maraviroc, a CCR5 inhibitor, reduced chemotaxis of the $CD4^+CD146^+CCR5^+$ T cell population toward CCL14. Mice that received CD146 shRNA–transduced human T cells did not lose weight, showed better survival, and had fewer $CD4^+CD146^+CCR5^+$ T cells and less pathogenic Th17 infiltration in the intestine, even compared with mice receiving maraviroc with control shRNA–transduced human T cells. Furthermore, the frequency of $CD4^+CD146^+CCR5^+$ Tregs was increased in GI-GVHD patients, and these cells showed increased plasticity toward Th17 upon ICOS stimulation. Our findings can be applied to early risk stratification, as well as specific preventative therapeutic strategies following HCT.

Introduction

Allogeneic hematopoietic cell transplantation (HCT) is the most validated immunotherapy able to cure hematological malignancies via the graft-versus-leukemia (GVL) activity of donor T cells (1, 2). Unfortunately, donor T cells also mediate damage to normal host tissues, potentially leading to acute graft-versus-host disease (aGVHD). aGVHD is currently diagnosed according to clinical symptoms and eventually confirmed by biopsies of the main target organs: skin, liver, and gastrointestinal (GI) tract (3–5). GI-GVHD specifically is an often fatal complication of HCT (6, 7), for which no prognostic blood biomarkers have been validated. Although several markers have been identified at the onset of GVHD and statistical scores have been developed based on markers measured upon the occurrence of clinical signs (8–14), only 2 markers so far (suppression of tumorigenicity 2 [ST2] and T cell immunoglobulin and mucin domain–containing 3 [TIM3]) were measured at day 14 after HCT and can be considered as potential early prognostic markers that predict the risk of future development of aGVHD and nonrelapse mortality (NRM) (10, 12). In contrast, regenerating islet-derived 3-α (REG3α), a GI-GVHD marker, is secreted by Paneth cells in the intestinal crypts and traverses into the bloodstream following damage to the intestinal mucosa barrier, suggesting that REG3α secretion is a relatively late event in GVHD (9, 12). Thus, the need for the discovery and validation of additional early GI-GVHD prognostic markers still exists.

In the present study, we sought to identify an early GI-GVHD marker using in-depth proteomic profiling. Here, we present the discovery of 2 proteins, CD146, and the chemokine CCL14 as well as a population of T cells expressing both CD146, which binds to other CD146 molecules through homophilic

Authorship note: W. Li, L. Liu, and A. Gomez contributed equally to this work.

Conflict of interest: S. Paczesny has a patent on "Methods of detection of graft-versus-host disease" licensed to Viracor-IBT Laboratories.

Submitted: January 25, 2016
Accepted: April 5, 2016
Published: May 5, 2016

Reference information:
JCI Insight. 2016;1(6):e86660.
doi:10.1172/jci.insight.86660.

interaction, and CCR5, the chemokine receptor of CCL14. CD146 is a cell adhesion molecule expressed at the intercellular junction of endothelial cells (ECs) and is therefore involved in heterophilic cell-cell interactions and angiogenesis (15, 16). CD146 expression has been shown to be higher in intestinal biopsies from patients with inflammatory bowel disease (17, 18). Human CD146 is also expressed on a small subset of effector memory T cells (19–22) and, through CD146-CD146 interactions, may recruit activated T cells to inflammation sites (23, 24). CCL14 is a recently identified chemokine constitutively expressed in many tissues, including normal and inflamed intestinal epithelial cells, and is a ligand of the chemokine receptor CCR5 expressed on T cells (25–28). CCR5 has been shown to be required for T cell migration into inflamed intestine in experimental models of GVHD and human alloreactions (29–31), and its blockade with maraviroc, a CCR5 small molecule inhibitor, prevented visceral GVHD in a clinical trial (32). In the present study, we applied proteomic profiling of presymptomatic GI-GVHD samples to identify potential soluble candidate proteins, which led to the discovery of CD146 and CCL14. Then, we tested the hypothesis that T cells exhibiting increased expression of their receptors (CD146 and CCR5), individually or in combination, could serve as cellular markers of GI-GVHD.

Identification of early cellular GI-GVHD biomarkers could be translated into clinical utility in predicting higher risk of developing GI-GVHD and subsequent NRM, which would allow for the application of preventative therapeutic strategies following HCT. In addition, such markers may or may not reflect the pathophysiology of GI-GVHD, and the second goal of our study was to explore this aspect. Finally, if the identified markers happen to be activation markers expressed on T cells, they could represent novel druggable targets.

Results

Proteomics analysis of presymptomatic GI-GVHD. To discover GI-specific candidate proteins prior to GVHD onset, we applied in-depth quantitative proteomics as previously described (9, 10, 33). Patient samples were collected prospectively before the onset of GVHD symptoms and then selected based on patients' GI-GVHD statuses. We compared pooled plasma taken 14 days prior to clinical manifestations from 10 patients who later developed GI-GVHD (labeled with a heavy isotope) and 10 controls without GVHD at matched time points (labeled with a light isotope). The isotopes allowed for comparison of relative concentrations of proteins between the groups. The 2 pools were subjected to tandem mass spectrometry. We then selected candidate proteins showing at least 1.5-fold greater expression in GI-GVHD samples versus non-GVHD samples (Supplemental Table 1; supplemental material available online with this article; doi:10.1172/jci.insight.86660DS1) that were not previously identified in proteomics experiments performed with the same platform and for which antibodies to their cellular receptors were available if an ELISA kit was not available. Two lead proteins emerged: (i) CD146, a cell adhesion molecule expressed on ECs particularly during inflammation (18) and on a subset of activated T cells (20, 22, 34), allowing their entry into the intestine through homophilic CD146-CD146 interactions (23, 24); and (ii) CCL14 that binds to the T cell chemokine receptor CCR5 (25, 26), which is known to facilitate T cell infiltration into the intestine (29, 30) and for which trafficking can be blocked by a CCR5 small molecule inhibitor in GI-GVHD patients (32).

Because these proteins had not been previously identified in proteomics experiments and antibodies for their receptors on T cells were available, we analyzed their expression profiles on peripheral blood (PB) cells from 214 HCT patients (93 with GI-GVHD [including patients who experienced GI-GVHD after skin GVHD], 48 without GVHD, 33 with non-GVHD enteritis, and 40 with skin GVHD) at the onset of symptoms at a median of 29 days after HCT or at similar time points from patients with non-GVHD enteritis or without GVHD. We used the same cohort as the published REG3α study (9), including patients who had PB cells available. Briefly, the cohort consisted of 4 groups: patients with newly diagnosed GVHD involving the GI tract (with or without other organ involvement) (GI-GVHD); patients tested at similar time points who never developed GVHD symptoms (no GVHD); patients with GI distress that was inconsistent with GVHD either by clinical or histologic criteria (non-GVHD enteritis); and patients who presented with isolated skin GVHD (skin GVHD). PB samples were collected at the time of symptoms in a time frame of 48 hours before or after treatment and at similar times after HCT in patients without GVHD. We also added phenotyping prior to GI-GVHD or non-GVHD enteritis for those patients with PB samples and enough cells available. Of note, the cohort is smaller, as PB cells were not collected when the patients were seen in the outpatient clinic, whereas plasma samples were. The patient characteristics are summarized in Supplemental Table 2. The causes of non-GVHD enteritis are detailed in Supplemental Table 3.

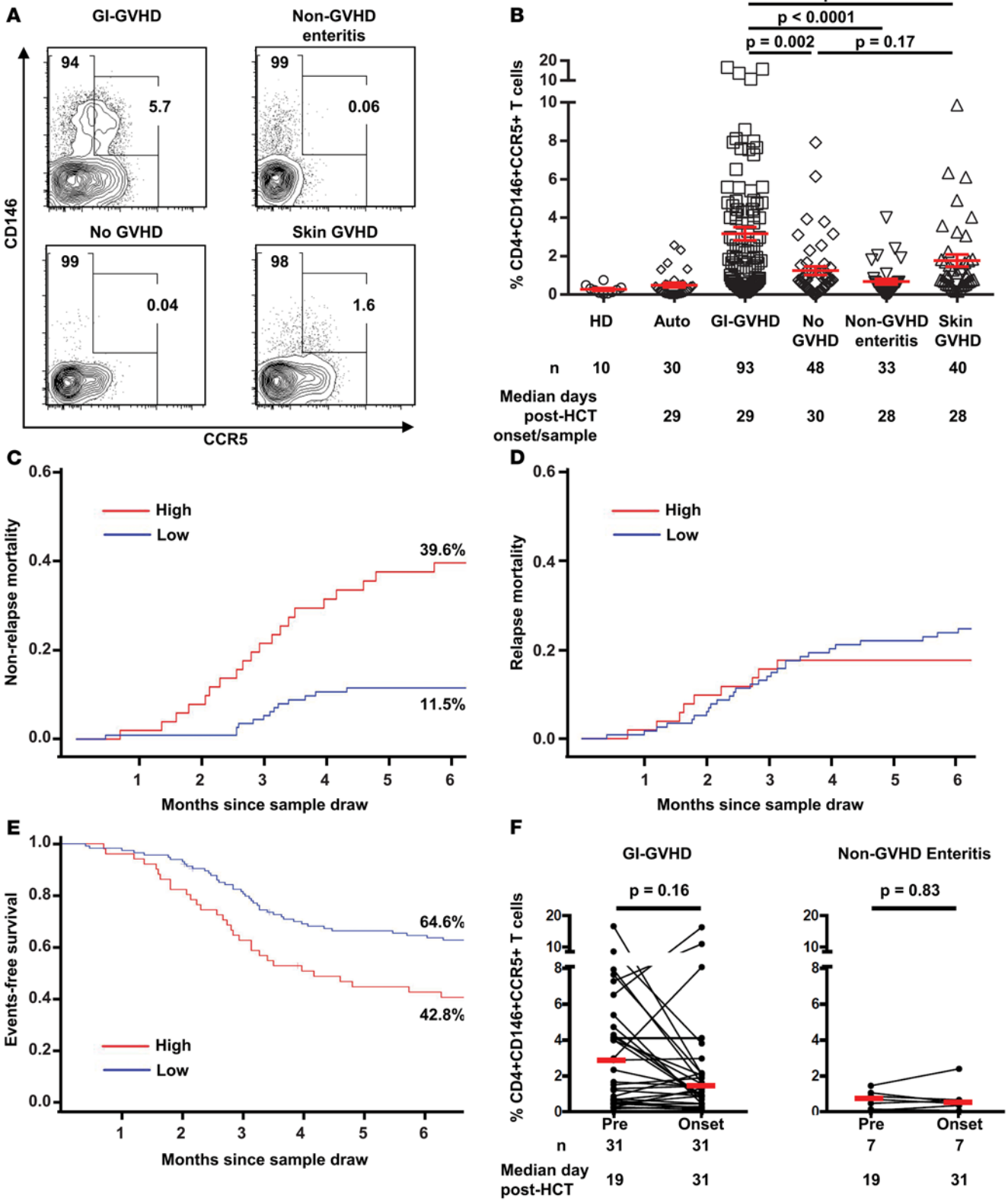
A
GI-GVHD
Non-GVHD enteritis
No GVHD
Skin GVHD
94
5.7
99
0.06
99
0.04
98
1.6
CD146
CCR5
B
p = 0.01
p < 0.0001
p = 0.002
p = 0.17
% CD4+CD146+CCR5+ T cells
HD
Auto
GI-GVHD
No GVHD
Non-GVHD enteritis
Skin GVHD
n 10 30 93 48 33 40
Median days post-HCT onset/sample 29 29 30 28 28
C
Non-relapse mortality
High
Low
39.6%
11.5%
Months since sample draw
D
Relapse mortality
High
Low
Months since sample draw
E
Events-free survival
64.6%
42.8%
High
Low
Months since sample draw
F
GI-GVHD
p = 0.16
Non-GVHD Enteritis
p = 0.83
% CD4+CD146+CCR5+ T cells
Pre
Onset
n 31 31 7 7
Median day post-HCT 19 31 19 31

Figure 1. A CD4$^+$CD146$^+$CCR5$^+$ T cell population in allogeneic HCT patients at GVHD onset and prior to GVHD onset. (**A**) Representative plots showing CCR5 and CD146 expression in samples from patients with GI-GVHD, without GVHD, with non-GVHD enteritis, and with skin GVHD. (**B**) CD4$^+$CD146$^+$CCR5$^+$ T cell frequencies in healthy donors (HD), autotransplant patients (Auto), and allogeneic patients. *n* and median post-HCT onset of signs or samples are shown below the graphs. The data are shown as mean ± SEM, 2-tailed Student's *t* tests. (**C**) Six-month nonrelapse mortality since sample draw in allogeneic HCT patients with symptoms (GI-GVHD, non-GVHD enteritis, and skin GVHD, *n* = 166) divided by low and high CD146$^+$CCR5$^+$ T cell frequencies. High-risk group in red (CD4$^+$CD146$^+$CCR5$^+$ T cell frequency ≥ 2.3%, *n* = 51) and low-risk group in blue (CD146$^+$CD146$^+$CCR5$^+$ T cell frequency < 2.3%, *n* = 115), *P* = 0.001, calculated for the overall curve. (**D**) Six-month relapse mortality since sample draw in the same population, *P* = 0.64. (**E**) Six-month event-free survival since sample draw in the same population, *P* = 0.002. (**F**) CD4$^+$CD146$^+$CCR5$^+$ T cell frequency in paired samples prior to GVHD onset in GI-GVHD patients (*n* = 31) with a median interval of 14 days between the first measurement and measurement at onset of disease and at matched time points in non-GVHD enteritis patients (*n* = 7), paired *t* test analysis. Cumulative incidence (**C** and **D**) and Kaplan-Meier analysis (**E**) used.

Conventional T cells were defined as CD4$^+$CD25^{lo}CD127$^+$ (see gating strategy in Supplemental Figure 1). The frequency of CD4$^+$CD146$^+$CCR5$^+$ T cells was greater in GI-GVHD patients than in patients without GVHD, with non-GVHD enteritis, or with skin GVHD (Figure 1, A and B). In addition, the absolute lymphocyte counts (ALCs) did not differ between groups, and the absolute count of CD4$^+$CD146$^+$CCR5$^+$ T cells was highly correlated to the CD4$^+$CD146$^+$CCR5$^+$ T cell frequency in the whole cohort (Spearman r = 0.63, $P < 10^{-4}$, Supplemental Figure 2). The frequency of T cells expressing only CD146 followed the same trend as the CD4$^+$CD146$^+$CCR5$^+$ T cells with slightly less significance (Supplemental Figure 3A), whereas the frequency of CD4$^+$ T cells expressing only CCR5, although different between the GI-GVHD and non-GVHD enteritis groups, was not different between the GI-GVHD and no GVHD or skin GVHD groups (Supplemental Figure 3B). The CD8$^+$ T cells in GI-GVHD patients did not express enough detectable CD146 (lower than that in healthy donors) for interpretation as cellular marker (Supplemental Figure 4). The CD4$^+$CD146$^+$CCR5$^+$ T cell frequency discriminated GI-GVHD from non-GVHD enteritis with an AUC of 0.84, which was more robust than the AUC of 0.79 obtained using the CD4$^+$CD146$^+$ T cell frequency (Supplemental Figure 5 and not shown). These data suggest that the CD4$^+$CD146$^+$CCR5$^+$ T cell frequency, better than the CD4$^+$CD146$^+$ T cell frequency, could be used as a possible diagnostic marker of GI-GVHD, particularly in comparison with non-GVHD enteritis, an often challenging clinical dilemma.

CD4$^+$CD146$^+$CCR5$^+$ T cells and patient outcomes. The strength of a marker is enhanced if it can be used not only for diagnosis but to predict patient outcomes. Therefore, we investigated whether the CD4$^+$CD146$^+$CCR5$^+$ T cell frequency correlated with maximum GVHD severity or the 6-month NRM from the time the blood sample was drawn. The CD4$^+$CD146$^+$CCR5$^+$ T cell frequency measured at GVHD onset was greater in patients who eventually developed GI-GVHD of maximum severity (Supplemental Figure 6). We next analyzed the impact of the CD4$^+$CD146$^+$CCR5$^+$ T cell frequency on the 6-month NRM in all patients with symptoms (GI-GVHD, non-GVHD enteritis, and skin GVHD). We found that the median CD4$^+$CD146$^+$CCR5$^+$ T cell frequency in patients with GI-GVHD (2.3%) could be used as a cut point for the risk of NRM within 6 months from the sample draw, with 39.6% of patients in the high-risk group experiencing NRM compared with only 11.5% of patients in the low-risk group (*P* = 0.001, Figure 1C). In contrast, the incidence of relapse mortality was comparable in the groups (Figure 1D). Moreover, the 6-month event-free survival rates were 42.8% and 64.6% among patients with high and low CD4$^+$CD146$^+$CCR5$^+$ T cell counts, respectively (*P* = 0.002, Figure 1E), suggesting that the CD4$^+$CD146$^+$CCR5$^+$ T cell count has prognostic value.

CD4$^+$CD146$^+$CCR5$^+$ T cells circulate before GI GVHD onset. A new risk factor improves diagnostic power only if it does not correlate with other known markers. Our previous proteomics experiments revealed correlations between REG3α and ST2 with GI-GVHD (9, 10), but here we found that these markers were not highly correlated with the CD4$^+$CD146$^+$CCR5$^+$ T cell population (Supplemental Figure 7A). We also analyzed the CD4$^+$CD146$^+$CCR5$^+$ T cell frequency in patients categorized according to the localization of GI symptoms: diarrhea versus nausea/vomiting. The double-positive T cell population distinguished GI-GVHD from non-GVHD enteritis regardless of symptom localization, suggesting the CD4$^+$CD146$^+$CCR5$^+$ T cell subset appears early in the GVHD process, given that nausea/vomiting symptoms usually precede diarrhea symptoms (Supplemental Figure 7B). Furthermore, the CD4$^+$CD146$^+$CCR5$^+$ T cell frequency was not correlated with GI histologic severity, suggesting that these cells are not a product of mucosa damage but rather systemic effectors (Supplemental Figure 7C). Based on these observations and the identification of CD146 and CCL14 in proteomics analysis of samples collected prior to the onset of clinical signs, we next explored the prognostic value of the CD4$^+$CD146$^+$CCR5$^+$ T cell frequency using 31 paired samples collected before GI-GVHD at a median of 19 days after transplantation and at onset of GI-GVHD. The CD4$^+$CD146$^+$CCR5$^+$ T cell population was found to circulate in PB at a median interval of 14 days prior to the occurrence of

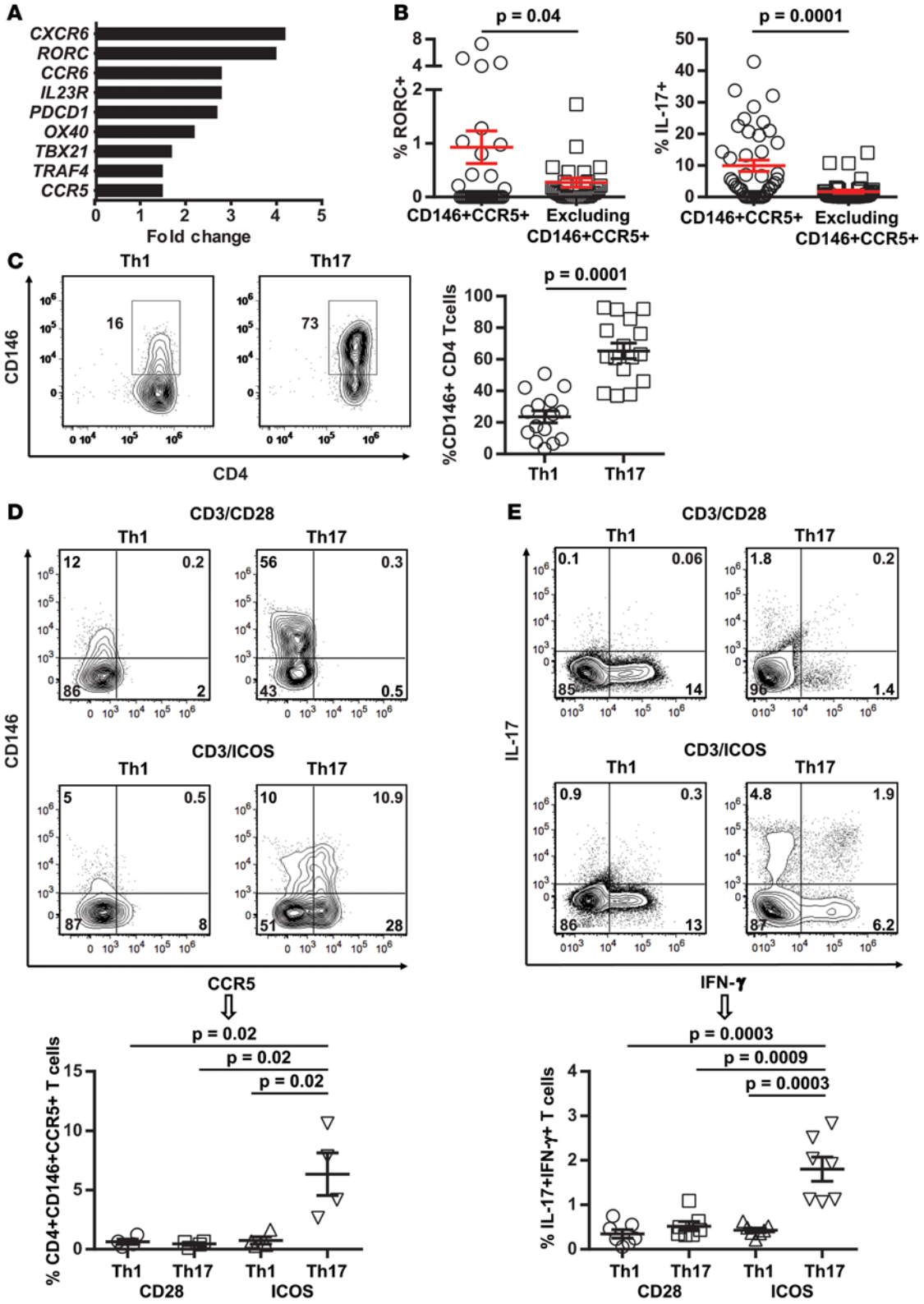

Figure 2. Th17-prone CD4⁺CD146⁺CCR5⁺ T cell population. (**A**) Differential transcriptomes in CD146⁺CCR5⁺ Tcons versus Tcons excluding this population. (**B**) RORC and IL-17 expression in patients' samples (n = 35 and 41, respectively). (**C**) Th1 or Th17 differentiation of naive T cells with anti-CD3/CD28 stimulation. Representative plots showing CD146 expression in CD4⁺ T cells and a dot plot depicting mean ± SEM values for frequency of CD146 (n = 16), 2-tailed Student's t test. (**D**) Th1 or Th17 differentiation of naive T cells with anti-CD3/CD28 or anti-CD3/ICOS stimulation. Representative plots of CD146 and CCR5 expression and a dot plot depicting mean ± SEM values for frequency of CD4⁺CD146⁺CCR5⁺ T cells (n = 4), 2-tailed Student's t test. (**E**) Representative plots showing IL-17 and IFN-γ coexpression in CD4⁺ T cells and a dot plot depicting mean ± SEM values for frequency of IL-17⁺IFN-γ⁺ T cells in the same 4 conditions as in **E** (n = 7), 2-tailed Student's t test.

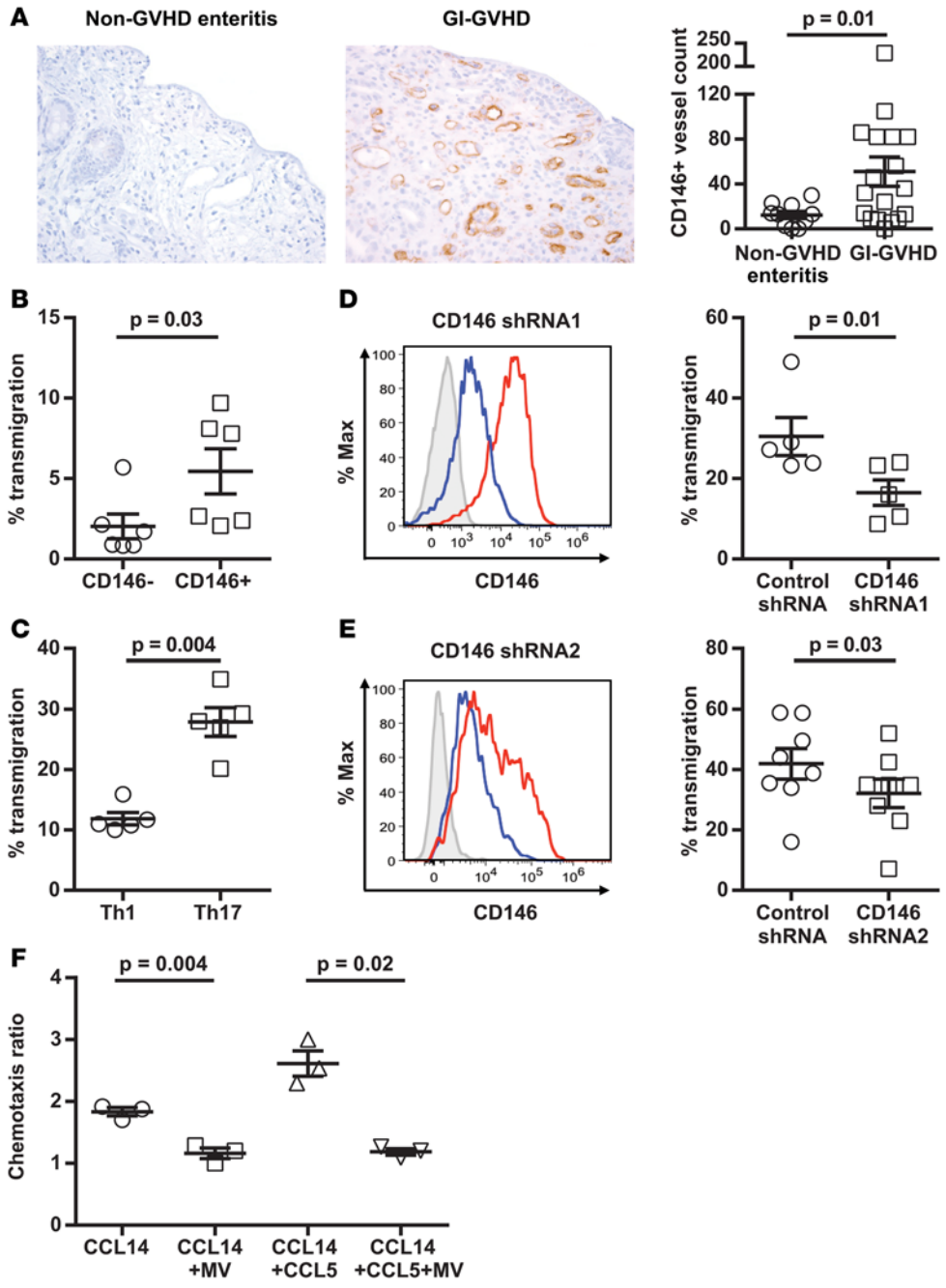

Figure 3. Endothelial CD146 expression in GI-GVHD colonic biopsies, transendothelial migration of CD4$^+$ T cell subsets and with CD146 knockdown, and chemotaxis of CD4$^+$CD146$^+$CCR5$^+$ T cells. (**A**) Immunohistochemical analysis of CD146 expression in colonic biopsies taken at onset of symptoms from non-GVHD enteritis patients and GI-GVHD patients (magnification ×200). Dot plot showing mean ± SEM values for CD146$^+$ vessel counts ×10, 2-tailed Student's *t* test from non-GVHD enteritis patients (n = 10) and GI-GVHD patients (n = 18). (**B**–**E**) Transendothelial migration of CD146$^-$ and CD146$^+$ T cells sorted from PB cells, Th1 and Th17 cells, Th17 cells with CD146 knockdown via CD146 shRNA1, or CD146 shRNA2. Representative flow cytometric histograms showing the efficiency of CD146 knockdown. Isotype control staining (gray) and CD146 staining of cells with the control shRNA (red) and CD146 shRNA (blue). Dot plots show mean ± SEM values for percentage of transmigrated CD4$^+$ T cells (n = 6 for **B**, n = 5 for **C**, n = 5 for **D**, and n = 8 for **E**), 2-tailed Student's *t* test. (**F**) CCR5-mediated chemotaxis of CD4$^+$CD146$^+$CCR5$^+$ T cells toward CCL14 or CCL14 and CCL5. The sorted double-positive cells were pretreated with maraviroc (MV) or vehicle control. Data are presented as mean ± SEM values (n = 3), paired *t* test.

GI-GVHD symptoms at a frequency not significantly different from that at onset, whereas the frequency of CD4$^+$CD146$^+$CCR5$^+$ T cells was not increased in non-GVHD enteritis patients at a median interval of 14 days prior to the occurrence of non-GVHD diarrhea symptoms (Figure 1F). We also analyzed the CD4$^+$CD146$^+$CCR5$^+$ T cell frequency in GI-GVHD patients over time after sampling (samples for 93 patients were collected at onset, and preonset samples for 31 patients were collected at time points between days 14 and 92 after HCT) and found no indication that this population varies over time in the blood of patients. Interestingly, 6 values over 10% were observed between days 19 and 27 after HCT (Supplemental Figure 8).

CD4$^+$CD146$^+$CCR5$^+$ T cells are Th17 prone. We then characterized the CD4$^+$CD146$^+$CCR5$^+$ T cell population and defined differential transcriptomes between sorted CD4$^+$CD146$^+$CCR5$^+$ T cells and T cells excluding this population (Supplemental Table 4). Transcription of RAR-related orphan receptor C (RORC), a transcription factor essential for Th17 development, was upregulated 4-fold, and this upregulation was confirmed at the protein level by intracellular staining of RORC and IL-17 in patient samples (Figure 2, A and B). Intracellular staining for Th1-transcription factor TBET in the same patient samples did not indicate

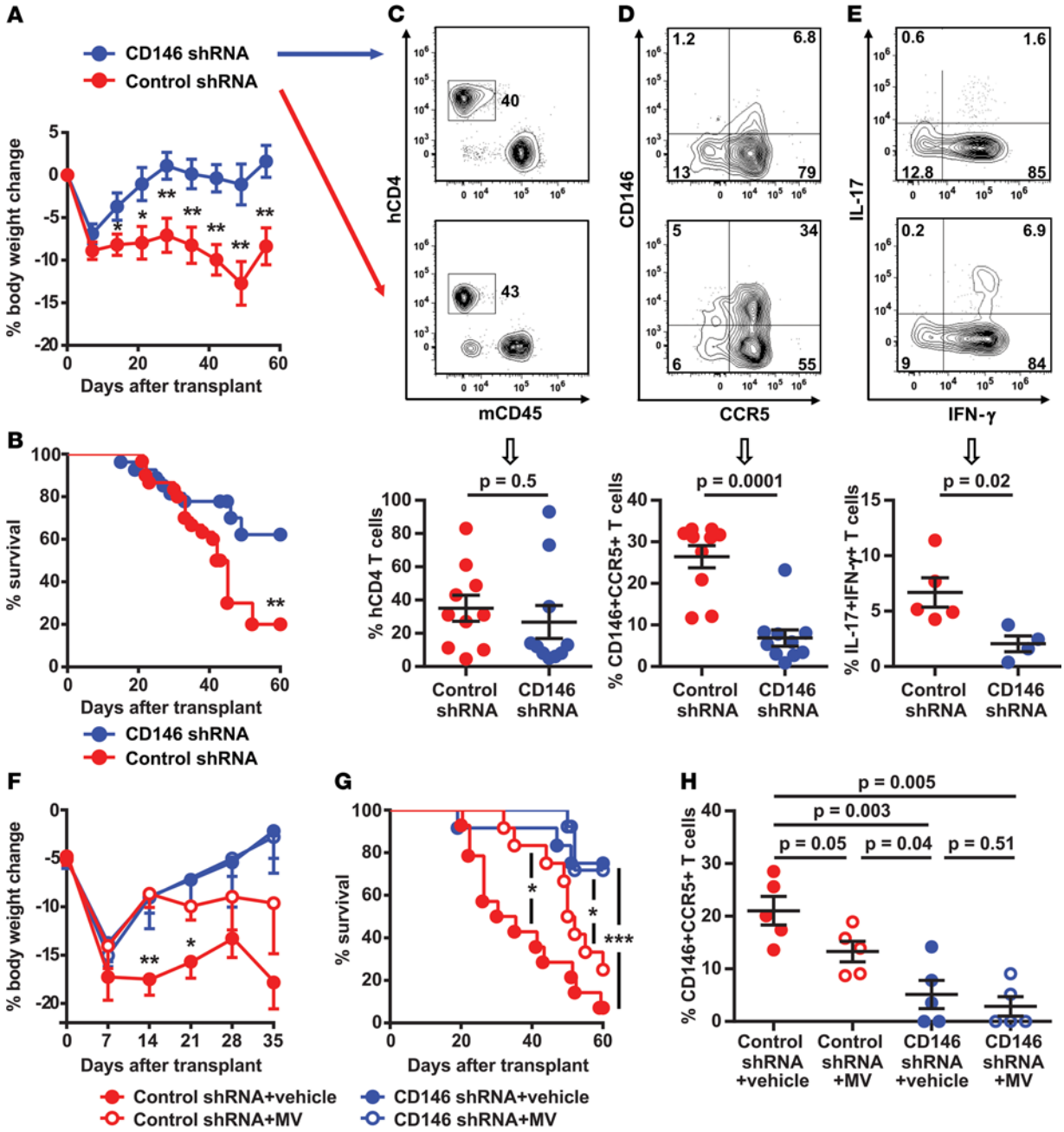

Figure 4. Donor human T cells with CD146 knockdown in a xenogeneic GVHD model. (**A**) Body weight loss of NSG mice transplanted with lentivirally transduced human CD4⁺ T cells. Control shRNA group (n = 8) and CD146 shRNA group (n = 9), 2-tailed Student's t test. (**B**) Kaplan-Meier survival curves. Control shRNA group (n = 30) and CD146 shRNA group (n = 27), log-rank test. (**C**) Human CD4⁺ T cell engraftment in spleen, (**D**) CD4⁺CD146⁺CCR5⁺ T cell frequency in the gut, and (**E**) Th17 cells coexpressing IL-17 and IFN-γ in the spleen. Mice were analyzed between days 30–45 after transplantation for **C**–**E**. Representative flow cytometric plots at the top and dot plots showing mean ± SEM values at the bottom, 2-tailed Student's t test. The data in **C** and **D** were from 10 mice per group. The data in **E** were from 5 mice in the control group and 4 mice in the CD146 group. (**F**) Body weight loss and (**G**) survival curves of NSG mice transplanted with CD146 shRNA or control shRNA lentivirus and treated with maraviroc (MV) or vesicle control, 2-tailed Student's t test for weight loss between control shRNA vs. control shRNA + MV and log-rank test for survival (n = 12 per group). (**H**) Human T cell infiltration in the gut of mice receiving transduced CD4⁺ T cells and MV or vehicle control. Mice were analyzed at day +35 after transplantation (n = 5 per group), 2-tailed Student's t test. $^*P < 0.05$, $^{**}P < 0.01$, $^{***}P < 0.001$.

significant upregulation (Supplemental Figure 9). The CD4⁺CD146⁺CCR5⁺ T cell population is also characterized by an effector memory phenotype defined by the absence of CD45RA and CCR7 (35) as compared with the T cell population excluding the double-positive population (Supplemental Figure 10). In the same transcriptomic profile, we looked at 9 Th17 stemness transcripts (36, 37) in the CD4⁺CD146⁺CCR5⁺ T cells versus T cells excluding this population and found no significant differences (Supplemental Table 5).

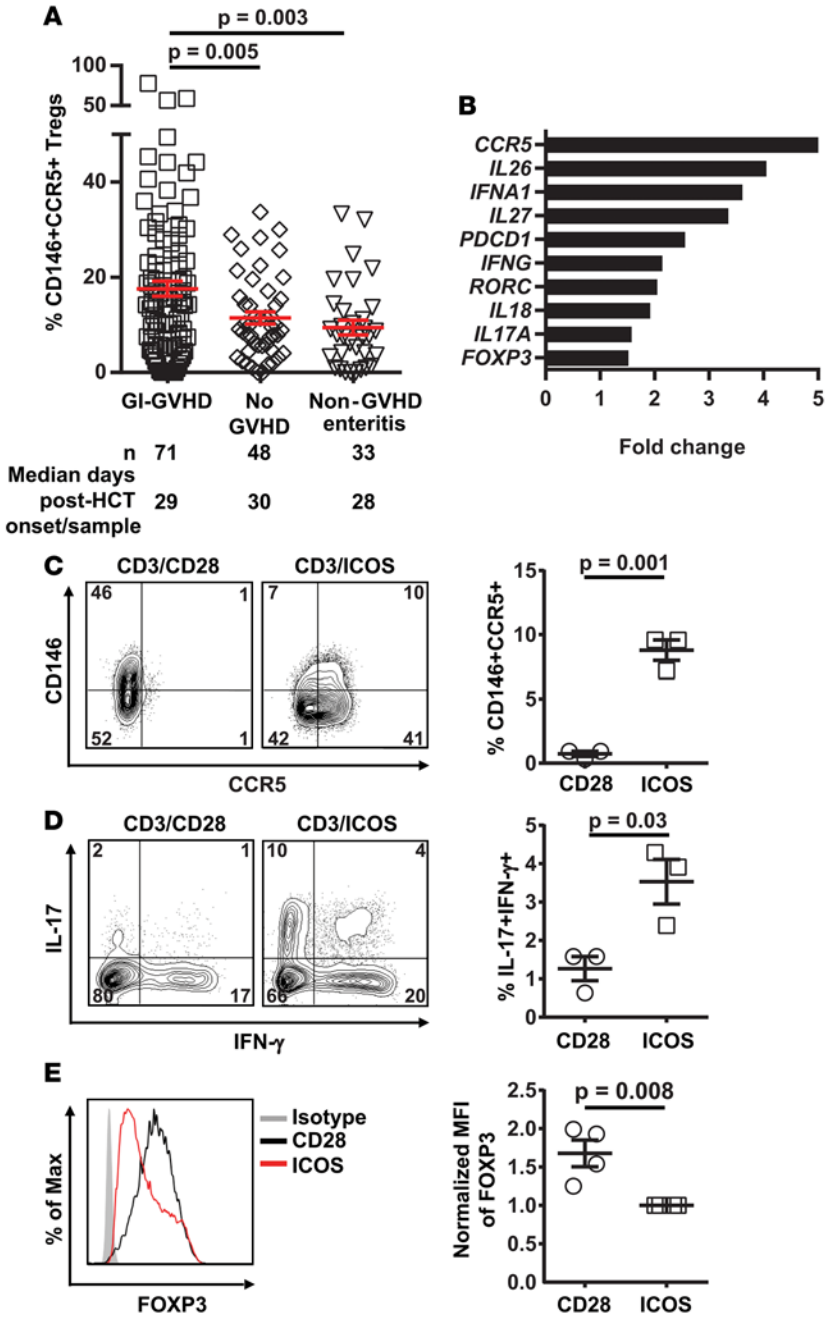

Figure 5. CD146⁺CCR5⁺ Tregs in allogeneic HCT patients at GVHD onset and ICOS-induced CD146⁺CCR5⁺ Tregs. (**A**) CD146⁺CCR5⁺ Treg frequencies in HCT patients. *n* and median post-HCT onset of signs or samples are shown below the graphs. The data are shown as mean ± SEM, 2-tailed Student's *t* test. (**B**) Differential transcriptomes in sorted CD146⁺CCR5⁺ Tregs vs. Tregs excluding this population. (**C**) Representative plots showing CD146 and CCR5 expression in Tregs stimulated with anti-CD3/CD28 or anti-CD3/ICOS beads, and a dot plot depicting mean ± SEM values for frequency of CD146⁺CCR5⁺ Tregs (*n* = 3), 2-tailed Student's *t* test. (**D**) Representative plots showing IL-17 and IFN-γ coexpression in Tregs, and a dot plot depicting mean ± SEM values for frequency of IL-17⁺IFN-γ⁺ T cells in the same 2 conditions as in **C** (*n* = 3), 2-tailed Student's *t* test. (**E**) Representative plots showing FOXP3 expression in Tregs stimulated with anti-CD3/CD28 or anti-CD3/ICOS beads, and a dot plot depicting mean ± SEM values for normalized mean fluorescence intensity (MFI) of the Tregs (*n* = 4), 2-tailed Student's *t* test. Isotype control staining in gray.

Consistent with data from patient samples, CD146 expression in in vitro Th17-differentiated cells was 3-fold greater than in Th1-differentiated cells (Figure 2C). We also verified that CD4⁺CD146⁺CCR5⁺ T cells were induced upon allogeneic reactivity (Supplemental Figure 11). ICOS stimulation is critical for the development of human Th17 cells (38), and we found that ICOS stimulation and Th17 differentiation conditioning induced the CD4⁺CD146⁺CCR5⁺ population (Figure 2D). CCR5 expression was not upregulated after activation by CD28 costimulation, which is consistent with previous findings (39). Importantly, this conditioning also increased the number of cells coexpressing IL-17/IFN-γ (Figure 2E).

Other Th17 markers, such as CD161, IL-23R, and CXCR6 (40–44), were all expressed at higher levels in T cells differentiated with Th17 conditioning and ICOS (Supplemental Figure 12A). Furthermore, we analyzed the following Th17 markers — IL-17/IFN-γ, GM-CSF, IL-22, CCR4, CCR6, CD161, CXCR6, and IL-23R — in the double-positive T cells as compared with the T cells excluding this population (Supplemental Figure 12B). Overall, these data show that the CD4⁺CD146⁺CCR5⁺ T cell population is Th17 prone and increased by ICOS stimulation, linking these cells to two known driving forces for the induc-

tion and amplification of the GVHD effector phase, which results in direct and indirect damage to host cells. Importantly and consistent with patient data, ICOS signaling did not induce significantly more $CD8^+CD146^+CCR5^+$ T cells than did CD28 signaling (Supplemental Figure 13A), which was in contrast to ICOS-induced generation of $CD4^+CD146^+CCR5^+$ T cells from conventional T cells (Tcons) (Supplemental Figure 13B). Together, our data are consistent with previously published findings demonstrating the involvement of Th17 cells in the pathogenesis of GI-GVHD (45–48).

Because it is technically impossible to sort enough double-positive cells from a single healthy donor buffy coat to perform functional experiments (mean ± SEM: 0.10% ± 0.02% of total cells or 0.26 ± 0.15 million $CD4^+CD146^+CCR5^+$ T cells, $n = 5$), and because the total $CD4^+CD146^+$ T cell population is sufficiently correlated with the double-positive T cell population, we performed additional experiments on sorted $CD146^+$ T cells (0.64% ± 0.09% of total cells or 1.53 ± 0.44 million $CD4^+CD146^+$ T cells after sorting from a single healthy donor buffy coat, $n = 11$), we focused on $CD146^+$ T cells for functional and in vivo studies. For this purpose, we analyzed their phenotype and found that mature $CD146^+$ T cells expressed equivalent amounts of IL-17 after in vitro differentiation under Th1 or Th17 conditions with CD28 or ICOS costimulation (Supplemental Figure 14). This result suggested that they are antigen experienced and Th17 prone before they acquire the CCR5 surface antigen and they could be used as a surrogate cell type for $CD4^+CD146^+CCR5^+$ T cells in efforts to decipher their mechanism in vitro.

CD146 endothelial expression is increased in GI-GVHD biopsies and Th17-polarized CD146 T cells preferentially migrate through the activated endothelium. Because the $CD4^+CD146^+CCR5^+$ T cell population circulates early after HCT and endothelial CD146 is overexpressed during inflammation (18), we hypothesized that, in response to transplant conditioning and cytokine release, alloreactive T cells express the double-positive population in parallel to increased CD146 expression in the intestinal endothelium and increased CCL14 release from the epithelium. This would allow $CD4^+CD146^+CCR5^+$ T cells to transmigrate across the endothelium via CD146-CD146 interaction and then to come in contact with the intestinal epithelium through chemotaxis to CCL14. To test the hypothesis that CD146 and CCL14 are upregulated in GVHD-activated intestine, we stained colonic biopsies of patients with non-GVHD enteritis and GI-GVHD for CD146 and CCL14. Significantly greater CD146 expression was observed on the endothelium of GI-GVHD patients (Figure 3A), and CCL14 expression also was increased in GI-GVHD, although not significantly (Supplemental Figure 15). Of note, $CD3^+CD146^+$ expression on T cells was not significantly altered (Supplemental Table 6). These results suggest that both endothelial and lymphocytic CD146 could play an important role in recruiting pathogenic T cells to the intestine. If our hypothesis is true, more $CD146^+$ and Th17-differentiated T cells should transmigrate through the activated endothelium as compared with $CD146^-$ and Th1 cells. Indeed, more $CD146^+$ or Th17 cells migrated through TNF-α–activated ECs in transwell assays (Figure 3, B and C). Lentivirally induced shRNA knockdown of CD146 in $CD4^+$ T cells led to a significant reduction in T cell transmigration (Figure 3D). To eliminate possible off-target effects, we verified these results with a second shRNA (Figure 3E). However, siRNA knockdown of CD146 on ECs did not reduce T cell transmigration (not shown), suggesting that CD146 on T cells, but not on ECs, is a key promoter of pathogenic T cell infiltration into GVHD target organs.

$CD4^+CD146^+CCR5^+$ T cells show increased chemotaxis toward CCL14 that is inhibited by maraviroc. We next evaluated the chemotaxis of $CD4^+CD146^+CCR5^+$ T cells to CCL14. CCR5 on T cells can bind both CCL14 and CCL5, but only CCL14 was identified in the proteomics experiment. Thus, we tested the chemotaxis of $CD4^+CD146^+CCR5^+$ T cells to CCL14 and $CCL14^+CCL5^+$ T cells. Chemotaxis of $CD4^+CD146^+CCR5^+$ T cells was significantly increased toward CCL14 and even more so toward both $CCL14^+CCL5^+$ T cells. This chemotaxis was inhibited by the CCR5 inhibitor maraviroc (Figure 3F), and this inhibition was similar to that previously shown with T lymphoblasts (28).

CD146 shRNA–transduced T cells reduce xenogeneic GI-GVHD. To evaluate the in vivo role of CD146 on T cells, we first used CD146 KO T cells in allogeneic murine GVHD models. Transfer of CD146 KO T cells had not previously been used in immune-mediated disease models. Unfortunately, the GVHD severity did not differ upon transplantation of these cells versus WT T cells (Supplemental Figure 16, A and B), which may be due to the low expression of CD146 on donor murine T cells compared with human T cells (Supplemental Figure 16C) as previously shown (49). We therefore transplanted donor human $CD4^+$ T cells, which express approximately 2% of CD146 (19) before lentiviral transduction, with CD146 knockdown achieved via lentiviral shRNA in the xenogeneic mouse GVHD model. CD146 expression in transduced $CD4^+$ T cells was significantly knocked down by the CD146 shRNA both at the time of transplantation and

at day 45 after transplantation (Supplemental Figure 17). In comparison with the control group, immunodeficient NOD/scid/IL-2Rγ$^{-/-}$ (NSG) mice transplanted with CD146 shRNA–transduced T cells did not lose weight (Figure 4A), had better survival (Figure 4B), showed similar human T cell engraftment (Figure 4C), had fewer CD4$^+$CD146$^+$CCR5$^+$ T cells in the intestine (frequencies and absolute counts, Figure 4D and Supplemental Figure 18, respectively), and had fewer IL-17/IFN-γ–coexpressing T cells (Figure 4E). We could not technically transfer double CD146 and CCR5 shRNA–transduced T cells; however, we next attempted to test the role of CCR5 inhibition by using the CCR5 inhibitor maraviroc in the xenogeneic model, as has been done in patients (32). We also compared its action with the control shRNA–transduced T cells and the CD146 shRNA–transduced T cells plus maraviroc. NSG mice transplanted with control shRNA–transduced T cells and treated with maraviroc for 21 days lost less weight than the untreated mice transplanted with control shRNA–transduced T cells (Figure 4F), showed improved survival (Figure 4G), and had less CD4$^+$CD146$^+$CCR5$^+$ T cell gut infiltration (Figure 4H). Transplantation of CD146 shRNA–transduced T cells also showed a decrease in the in vivo production of IL-17/IFN-γ by CD4$^+$ CD146$^+$CCR5$^+$ T cells, whereas treatment with maraviroc had no effect on the in vivo production of IL-17/IFN-γ by the CD4$^+$CD146$^+$CCR5$^+$ T cells (Supplemental Figure 19). There were no differences in body weight, survival, or CD4$^+$CD146$^+$CCR5$^+$ T cell infiltration in the intestine between NSG mice transplanted with CD146 shRNA–transduced T cells and those transplanted with CD146 shRNA–transduced T cells and treated with maraviroc (Figure 4, F–H), possibly suggesting that CCR5 is acquired by the Th17-prone CD146 T cells during GVHD development.

CD4$^+$CD146$^+$CCR5$^+$ Treg frequency is increased in GI-GVHD patients. Tregs are crucial for the inhibition of GVHD development (50). In our study, the frequency of total Tregs defined by CD25$^+$CD127$^-$FOXP3$^+$ on CD4$^+$ T cells (see gating strategy in Supplemental Figure 1) was significantly decreased in GI-GVHD patients compared with patients with non-GVHD enteritis (P = 0.006) and patients without GVHD (P = 0.04) as previously reported (refs. 51–53 and Supplemental Figure 20). However, the frequency of CD146$^+$CCR5$^+$ Tregs was increased in GI-GVHD patients as compared with patients with non-GVHD enteritis (P = 0.003) and patients without GVHD (P = 0.005; Figure 5A). We further characterized the CD146$^+$CCR5$^+$ Tregs using NanoString analysis and found that, although they still express FOXP3, they also express inflammatory molecules such as IL-26, IFN-α, IL-27, IFN-γ, RORC, IL-18, IL-17A, and the exhaustion marker PD-1 (Figure 5B and Supplemental Table 7). Expression of IFN-γ, IL-17, and PD-1 in the double-positive Tregs as compared with the Tregs excluding CD146$^+$CCR5$^+$ cells was confirmed at the protein level by flow cytometry (Supplemental Figure 21). These data suggest that the CD146$^+$CCR5$^+$ Tregs might show increased plasticity toward Th17. To explore this hypothesis, we differentiated human Tregs in CD28 or ICOS conditions and found that ICOS stimulation increased the frequency of CD146$^+$CCR5$^+$ T cells (Figure 5C), increased the percentage of cells coexpressing IL-17/IFN-γ (Figure 5D) among the Tregs, and decreased the intensity of FOXP3 expression (Figure 5E). However, ICOS-expanded Tregs had similar suppressive activity as CD28-expanded Tregs (Supplemental Figure 22).

Discussion

The first aim of this study was to identify proteins and/or cellular risk factors that can predict future GI-GVHD and NRM before the development of symptoms, which would allow preemptive therapy and more stringent monitoring in high-risk patients. Equally important to identifying high-risk patients is the identification of patients who are at low risk of developing aGVHD, as these patients could avoid exposure to immunosuppressive regimens and thereby experience reduced toxicity. Herein, we used a mass spectrometry–based technique to unambiguously identify candidate plasma proteins expressed in GI-GVHD, the primary cause of NRM after HCT. Diarrhea is common after HCT and can be caused by a variety of stimuli, but because the consequences of GVHD are serious, physicians initiate treatment of suspected GVHD often without a bona fide confirmed diagnosis. For the time period before or at the onset of symptoms of GVHD with GI involvement, the principal findings of our study are that: (i) measurement of CD4$^+$CD146$^+$CCR5$^+$ T cells and CD146$^+$CD4$^+$ T cells frequencies and counts had prognostic utility in predicting development of GI-GVHD and (ii) predictive value for 6-month NRM and event-free survival. The high frequency of CD4$^+$CD146$^+$CCR5$^+$ T cells circulating before the occurrence of GI symptoms and as early as day 14 after HCT suggests that their "expansion" is an early event in the pathogenesis of GI-GVHD. Furthermore, the majority of patients with paired samples had stable or decreasing frequencies of CD4$^+$CD146$^+$CCR5$^+$ T cells in the blood, which could suggest these cells have already homed to the gut, resulting in their decrease

in number in the blood between the two time points (14 days on average). The frequencies of $CD4^+$ $CD146^+CCR5^+$ T cells were not correlated with REG3α and ST2, proteins that have been previously linked to GI-GVHD development (9, 10), suggesting that this T cell population might be an independent indicator of GI-GVHD, likely via a different biological mechanism. We believe that our results can improve the assessment of GVHD risk before the development of clinical signs of GI-GVHD; however, additional independent cohorts will be required to establish the frequency of $CD4^+CD146^+CCR5^+$ T cells as a biomarker. A generalizable definition of high risk has yet to be developed and will require larger studies.

The second aim of this study was to explore whether this T cell population is a mechanistic marker, meaning that it is involved in the pathophysiology of GI-GVHD. First, CD146 was found highly upregulated in GI-GVHD endothelium, which is consistent with findings in other inflammatory GI diseases (17, 18, 24). We did not observe a clear difference in CD146 expression on the endothelium according to a high- or reduced-conditioning regimen–intensity or immune suppression–induced damage among GI-GVHD and non-GVHD enteritis colonic biopsies, although we need to be cautious in drawing conclusions due to the small sample size. Second, the double-positive T cell population identified in our study traffics more efficiently through the endothelium, and our results demonstrate that CD146 on T cells, but not on ECs, is a key promoter of pathogenic T cell infiltration into GVHD target organs. This is in contrast to previous findings that targeting endothelial CD146 and not T cells decreases lymphocyte infiltration through the blood-brain barrier in an experimental autoimmune encephalomyelitis model (EAE model) or through the intestinal endothelium in colitis-associated carcinogenesis (24, 54). In contrast to our original hypothesis, our data showed that there are no homophilic CD146-CD146 interactions; thus, the most logical potential receptor on the endothelium is laminin-411, as it has been shown to be the vascular ligand for CD146 and to facilitate Th17 cell entry in the CNS in EAE (55). Third, the high affinity CCR5 ligand CCL14 tended to be increased in GI-GVHD patients' colonic cells. CCL14 is constitutively expressed and secreted by multiple tissues and is present in high concentrations in plasma (25). However, proteolytic processing of CCL14 is required to generate high-affinity binding to CCR5 (28), and it is possible that CCL14 is efficiently processed only in the GI tract. Furthermore, we showed that CCR5 played a functional role in driving chemotaxis of $CD4^+CD146^+CCR5^+$ T cells toward CCL14. We also showed that GVHD was improved in mice that received maraviroc with shRNA control human T cells but less so in mice that received only CD146 shRNA–transduced human T cells. Several studies have explored the role of CCR5 in alloreactivity with data that are either concordant or discordant to our findings as discussed below. In the pathogenesis of human aGVHD, CCR5-mediated alloreactivity on Tcons enhances aGVHD (31), and the CCR5 antagonist maraviroc limits GI-GVHD in recipients of allo-HCT (32). However, in another study using experimental models (29), the authors clearly showed that GVHD occurred more commonly in mice receiving $CCR5^{-/-}$ Tregs than in WT mice. Another study showed that the frequency of high CCR5-expressing Tregs was significantly greater in patients without GVHD than in those with GVHD before day 100 (56). Based on our data, we believe that the role of the double-positive $CD146^+CCR5^+$ Tregs is important but less than the double-positive Tcons because although they are plastic toward Th17, they remain suppressive (Supplemental Figure 22). Fourth, we showed that the $CD4^+CD146^+CCR5^+$ T cell population is Th17 prone and antigen experienced, which is consistent with previously published reports (45–48). The $CD4^+$ $CD146^+CCR5^+$ T cell population also displayed a molecular signature of pathogenic Th17 cells (ref. 44 and Supplemental Table 8). Fifth, the role of ICOS signaling in generating this population must be highlighted. ICOS stimulation through ICOS ligands, in concert with the cytokine milieu, critically dictates the fate of human Th17 cells (38). Similarly, we found that ICOS stimulation and Th17 differentiation conditioning induced the $CD146^+CCR5^+$ Tcons that coexpress IL-17/IFN-γ. We also found that $CD146^+CCR5^+$ Tregs could be induced by ICOS/ICOS ligand signaling and that, as a result, these cells produced IL-17 and exhibited decreased FOXP3 expression as described previously (38, 57). These results suggest that these Tregs exhibit increased plasticity — flexibility from one Th lineage to the other caused by changes in the environment — toward Th17, a phenomenon that is currently widely accepted (58). Based on this finding, it would be interesting to determine if patients with GI-GVHD have antigen-presenting cells (APCs) that express ligands for ICOS and CD28 on their cell surface and if it is due to host preconditioning, cytokine release, alloreactivity, and perhaps the microbiome. Indeed, host preconditioning with total body irradiation was recently shown to induce ICOS ligand expression on APCs (59). This requires further exploration in experimental models, given that studying recipient antigen presentation in patients is difficult (beyond correlative studies that are imperfect).

Finally, the results of our study have several therapeutic implications because this population has potential as a druggable target, such as has been shown recently for the biomarker ST2 (60, 61). Importantly, because both $CD146^+CCR5^+$ Tcons and Tregs are increased, they can potentially be targetable by the same systemic drugs. In addition, because Th17 and IL-17–expressing Tcon (Tc17) induce GVHD without antileukemic effects (62, 63), these interventions should be able to separate GVHD and the graft-versus-tumor effect. The first potential target is CCR5. Maraviroc already has been shown to improve GI-GVHD when administered in a prophylactic regimen (32). The second potential target is CD146. Human and murine anti-CD146 monoclonal antibodies have been used to block CD146 adhesion of Th17 cells in human brain endothelium (64) and in EAE and colitis (24, 54). The third potential target is the IL-17–expressing T cells that could be blocked by with either anti–IL-17 antibodies or RORC small molecule inhibitors that can be used in both mice and humans. The different mechanisms possibly involved in targeting the IL-17 pathway for the prevention of GVHD have recently been reviewed (65). The fourth potential target is the ICOS/ICOS ligand pathway, which can be blocked by anti-ICOS inhibitors. Anti–murine-ICOS has been successfully used to alleviate murine GVHD (66) and a syngeneic mouse model of melanoma transplanted with Tc17 (59). Different clones of anti–human-ICOS have been successfully used to ameliorate GVHD in SCID mice grafted with human PBMCs (67) and in the context of tumoral microenvironment (68).

We conclude that early measurement of the discovered $CD4^+CD146^+CCR5^+$ T cell population in the blood may allow identification of patients at increased risk for GI-GVHD and thus facilitate preemptive intervention via personalized medicine. This ICOS-stimulated, Th17-prone $CD4^+CD146^+CCR5^+$ T cell subset offers opportunities for potential therapeutic targets in GI-GVHD — such as CD146, RORC, and ICOS — in addition to the already targetable CCR5 that has been shown to alleviate GVHD (32).

Methods

Patients and samples. Heparinized PB cells were collected weekly during the first 4 weeks and then monthly after HCT, as well as at the onset of clinical key events (symptoms of GVHD or skin rash or non-GVHD enteritis).

All patients received pharmacologic GVHD prophylaxis with at least 2 agents, including a calcineurin inhibitor (>90% received tacrolimus). PB cells were isolated by density gradient separation and stored frozen at –120°C in liquid nitrogen. All patients received a T-replete graft and GVHD prophylaxis. Samples were not analyzed if methylprednisolone at a dose higher than 1 mg/kg was administered 48 hours or more before sample collection. Clinical data abstraction was aided by use of the electronic medical record search engine (EMERSE) (69).

Proteomics work flow. We used an unbiased top-down proteomic approach based on high-resolution mass spectrometry (Intact Protein Analysis System) as a discovery engine to identify candidate proteins followed by high-throughput sandwich enzyme–linked immunosorbent assay to validate the candidate proteins as reported previously (9, 10, 33)

Multicolor flow cytometry of patients' cells. Phenotyping of cell surface markers on frozen PB cells was performed using antibodies to CD4 (clone OKT4), CD25 (clone 2A3), CD127 (clone HIL-7R-M21), CD146 (clone P1H12), CCR5 (clone 2D7), CD45RA (clone HI100), and CCR7 (clone 3D12) (all from BD Biosciences). Intracellular staining of transcription factors (RORC, clone Q21-559, and TBET, clone 4B10) and cytokines (IL-17, clone eBio64DEC17, and IFN-γ, clone 4S.B3) was performed after fixation and permeabilization according to the manufacturer's recommendations using the buffer set (eBioscience). Tcons were defined as $CD4^+CD25^{lo}CD127^+$, and Tregs were defined as $CD4^+CD25^+CD127^-FOXP3^+$. Flow cytometric analysis was performed using an 8-color Canto II flow cytometer (BD Biosciences) and FlowJo software (Tree Star Inc.). Absolute counts of T cell subsets were calculated by multiplying the frequency of T cells among lymphocytes by the ALC obtained using the automated method.

IHC. Biopsies from GI-GVHD and non-GVHD enteritis patients were obtained per institutional guidelines. GVHD was confirmed by duodenal or colonic biopsy in 61 of 71 GI-GVHD patients. Biopsies were graded as described previously (70). CD146 and CCL14 monoclonal antibodies (clone sc-374556 and sc-28388, respectively) were purchased from Santa Cruz Biotechnology Inc. Immunostaining was performed by the tissue core of the University of Michigan Comprehensive Cancer Center for a subset of 18 GI-GVHD and 10 non-GVHD enteritis patients after HCT. All stained GI sections were coded, and 2 pathologists counted positive cells or positive blood vessels per ×10 optical field in a blinded manner at ×400 magnification.

Transcriptome analysis after cell sorting. Human leukopaks from healthy donors were purchased from the Central Indiana Blood Center under an IRB-approved protocol. PB cells were isolated by Ficoll (GE

Healthcare) density gradient centrifugation and stained with fluorescent-conjugated antibodies against CD146, CD4, CD8 (clone SK1, eBioscience), CD25, CCR5, and CD127. Stained cells were sorted for 2 populations ($CD146^+CCR5^+$ cells and cells excluding $CD146^+CCR5^+$) from the gated Tcons ($CD4^+CD25^{lo}CD127^+$) or Tregs ($CD4^+CD25^{hi}CD127^-$). The nCounter GX Human Immunology Kit (NanoString Technologies), which includes more than 500 clinically relevant immune genes, was used in our study. NanoString analysis was performed with the nCounter Analysis System.

T cell differentiation. T cells were purified from PB cells prepared from fresh leukopaks as described above. Naive $CD4^+$ T cells were negatively selected using a naive $CD4^+$ T cell isolation kit (Miltenyi Biotec). Total $CD4^+$ and $CD8^+$ T cells were isolated using $CD4^+$ or $CD8^+$ T cell isolation kits (Miltenyi Biotec). Tcons were positively selected with CD4 microbeads after depletion of CD25 cells with CD25 microbeads (Miltenyi Biotec). $CD4^+CD146^+$ and $CD4^+CD146^-$ T cells were purified using CD146 microbeads (Miltenyi Biotec) from negatively selected total $CD4^+$ T cells. Purified T cells were activated with anti-CD3/CD28 or anti-CD3/ICOS antibody–coated Dynabeads M-450 Tosylactivated (Invitrogen) at a bead/cell ratio of 1:5. For Th1 differentiation, IL-2 (2 ng/ml), IL-12 (10 ng/ml), and neutralizing antibodies against IL-4 (10 μg/ml) were added. All antibodies were obtained from eBioscience unless otherwise indicated. For Th17 differentiation, IL-1β (20 ng/ml), IL-6 (30 ng/ml), IL-23 (30 ng/ml), TGF-β (2 ng/ml), and neutralizing antibodies against IL-4 (5 μg/ml) and IFN-γ (2 μg/ml) were added. Exposure to differentiating cytokines (all from R&D Systems) and antibodies was maintained throughout the 7-day culture period.

In vitro Treg stimulation and suppression assays. $CD4^+CD25^+CD127^-$ T cells were purified from PB cells prepared from fresh leukopaks using the $CD4^+CD25^+CD127^-$ Regulatory T Cell Isolation Kit II (Miltenyi Biotec). For stimulation of Tregs, 0.1×10^6 T cells were plated in 96-well round bottom plates and stimulated with anti-CD3/CD28 or anti-CD3/ICOS antibody–coated Dynabeads in the presence of 500 U/ml IL-2. After 8–9 days, the stimulation beads were removed from Tregs before further analysis. For Treg suppression assays, 0.1×10^6 CFSE-labeled Tcons were activated with anti-CD3/CD28 beads and cultured with or without increasing numbers of anti-CD3/28 or anti-CD4/ICOS-expanded Tregs. After 3 days, proliferation of the responder Tcons was analyzed by flow cytometry.

Mixed lymphocyte reactions (MLRs). PB cells were prepared from healthy donors. In an allogeneic MLR, PB cells from one donor were irradiated at 3,000 cGy and mixed in a 1:1 ratio with PB cells or purified $CD4^+$ T cells from another donor. For autologous MLRs, irradiated PB cells were mixed with nonirradiated PB cells from the same donor. Cells were cultured for 8 days before analysis.

Flow cytometry for in vitro assays. Differentiated T cells or MLR cells were analyzed for cell surface expression of CD4, CD146, CCR5, CD161 (clone HP-3G10, eBioscience), CXCR6 (clone 56811, R&D Systems), and IL-23R (clone 218213, R&D Systems). For intracellular cytokine staining of IFN-γ, IL-17, IL-22 (clone IL22JOP) and GM-CSF (clone DAVKAT) (all from eBioscience), cells were stimulated with PMA (50 ng/ml; Sigma-Aldrich), ionomycin (1 μg/ml; Sigma-Aldrich), and brefeldin A (3 μg/ml, eBioscience) for 5 hours. Intracellular cytokines were stained with an intracellular fixation and a permeabilization buffer set (eBioscience). Stained cells were analyzed using an Attune Flow Cytometer (Invitrogen) and FlowJo software.

Lentiviral shRNA-mediated knockdown of CD146 on $CD4^+$ T cells. The pCL2EGw.THPC lentiviral vector used to generate CD146 shRNA and control shRNA contains a viral spleen focus forming (SFFV) promoter and a histone 1 promoter driving enhanced GFP and shRNA expression, respectively. To generate shRNA directed against CD146, the following 3 target sequences of the human CD146 gene were inserted between the Mlu I and Cla I sites of pCL2EGw.THPC: shRNA1 5′-GGAACTACTGGTGAACTAT-3′, shRNA2 5′-AGAGCGAACTTGTAGTTGA-3′, and shRNA3 5′-CCAACGACCTGGGCAAAAA-3′, which was used as a negative control shRNA because shRNA3 had no effect on CD146 expression on $CD4^+$ T cells.

To produce lentiviral particles, the CD146 shRNA or the control shRNA vector was cotransfected with the pCD/NL-BH helper plasmid and the pczVSV-G envelope plasmid into human embryonic kidney cells (HEK293T, ATCC, CRL-3216) as described previously (71). To knockdown CD146 expression on Th17-differentiated T cells with CD146 shRNA1, naive $CD4^+$ T cells were stimulated with anti-CD3/CD28 beads under Th17 conditions for 24 hours and transduced with CD146 and control shRNA lentivirus immobilized on Retronectin-coated 24-well plates (72). Beyond 6 days after infection, the Th17 cells were restimulated with anti-CD3/CD28 beads under Th17 conditions for 6 more days to achieve maximal knockdown. To knock down CD146 expression on Th17-differentiated T cells with CD146 shRNA2, naive $CD4^+$ T cells were stimulated with anti-CD3/ICOS beads under Th17 conditions for 24 hours, transduced with the CD146 and control shRNA lentivirus, and cultured for 5 additional days. Transduced cells were

then sorted based on GFP expression and used for in vitro assays. For in vivo functional analysis of lymphocytic CD146, $CD4^+$ T cells were preactivated with anti-CD3/CD28 beads and IL-2 (20 U/ml) for 24 hours, infected with CD146 and control shRNA lentivirus as described above, and expanded in the presence of IL-2 for 4–6 days. Then, GFP-expressing cells were sorted.

siRNA-mediated CD146 knockdown in HUVECs. The Silencer Select siRNA targeting the human CD146 gene (s8573, sense strand 5′-GGAACUACUGGUGAACUAUtt-3′ and antisense strand 5′-AUAGUUCACCAGUAGUUCCtg-3′) and the Silencer Select Negative Control No. 1 siRNA were obtained from Invitrogen and transfected into HUVECs using the TransIT-TKO Transfection Reagent from Mirus Bio according to the manufacturer's instructions. The HUVEC line was purchased from ATCC (PCS-100-010). Four days after transfection, significant reduction of CD146 was achieved, and the cells were used for the transmigration experiments.

Transmigration assays. The transmigration of T cells through human microvascular ECs (HMVECs) (Lonza Biosciences, CC-2543) was assayed using transwells with a 3-μm pore size (CoStar) and HMVECs between passages 7–10. HMVECs (2×10^4) were grown on 50 μg/ml collagen-coated transwell inserts in EGM-2MV medium (Lonza Biosciences) for 3 days, followed by treatment with fresh medium containing TNF-α (10 ng/ml, Sigma-Aldrich) for 24 hours. FACS-sorted $CD146^+$ and $CD146^-$ cells from fresh $CD4^+$ T cells among healthy donor PB cells, Th1 cells, or Th17 cells or sorted GFP^+ lentivirally transduced Th17 cells (1×10^5) were added to the top chamber and left to transmigrate through the HMVEC monolayers for 24 hours. T cells that migrated to the lower chamber were then collected and counted. The percent that transmigrated was calculated as the ratio of the number of transmigrated T cells to the number of input T cells × 100. Transmigration experiments were performed in duplicate.

Chemotaxis assay. MLR cultures were stained with antibodies against CD146 and CCR5 (clone REA245, Miltenyi Biotec) and sorted for $CD4^+CD146^+CCR5^+$ T cells. After culture in medium supplemented with 4 U/ml IL-2 overnight, cells were washed and preincubated with the CCR5 antagonist maraviroc (10 μM, Selleck Chemicals) or DMSO control for 30 minutes at 37°C in chemotaxis medium (RPMI-1640 and 0.5% BSA). Approximately 0.5×10^5 to 1×10^5 cells were added to the top chamber, and 600 μl of chemotaxis medium with or without 100 nM CCL14 (Met-[Gly28-Asn93], BioLegend) or a mixture of CCL14 and 50 nM CCL5 (BioLegend) was added to the bottom chamber of a 24-well Transwell system (polycarbonate filter with 3-μm pore size, CoStar). After incubation for 6 hours at 37°C, cells from the lower compartment were collected and counted by flow cytometry. Chemotaxis is represented as the ratio of the number of T cells migrating toward chemokines to the number of cells that underwent spontaneous migration.

CD146 KO donor T cells in murine allogeneic aGVHD models. T cells from the CD146 KO mice and WT controls (8–20 weeks of age) on the $H\text{-}2^b$ background (73) were provided for this study by Hong Wei Chu (National Jewish Health, Denver, Colorado, USA) and used to induce GVHD in 2 established murine models as previously described (74). Briefly, Balb/c ($H\text{-}2^d$, MHC-mismatched) and C3H.SW ($H\text{-}2^b$, minor histocompatibility antigen–mismatched) (8–12 weeks of age) recipient mice received 900 and 1,100 cGy irradiation, respectively, on day –1. Recipient mice were injected i.v. with T cell depleted (TCD) BM cells (5×10^6) from WT mice together with either WT or KO splenic T cells (1×10^6 WT or CD146 KO B6 T cells for Balb/c and 2×10^6 for C3H.SW) on day 0. Mice were housed in sterilized microisolator cages and maintained on acidified water (pH < 3) for 3 weeks as described previously (75). Mice were monitored for survival daily, assessed for clinical GVHD scores weekly as described previously (76), and euthanized when the clinical scores reached 6.

Human-to-mouse xenogeneic model of GVHD with CD146 or control shRNA knockdown human T cells. Immunodeficient NSG mice (8–14 weeks of age) were obtained from the In Vivo Therapeutics Core at the Indiana University Simon Cancer Center, housed under specific pathogen-free conditions, and maintained on food supplemented with Uniprim and acidic water. All procedures were performed in compliance with protocols approved by the institutional animal care and use committee and institutional biosafety committee. Twenty-four hours after sublethal irradiation at 300–350 cGy, NSG mice were injected i.v. with $1–2 \times 10^6$ sorted human $CD4^+$ T cells lentivirally transduced with the CD146 or control shRNA vector. In some experiments, maraviroc dissolved in 2 μl DMSO at a concentration of 100 mg/ml, or an equal volume of DMSO alone (vehicle) was diluted in 200 μl PBS and injected into mice i.p. (10 mg/kg) once daily from the day before T cell transplantation until 21 days afterward. Mice were monitored daily for survival and scored twice per week for GVHD signs as described above.

Spleen and small and large intestines were harvested from transplanted NSG mice. Single cell suspension of spleens was prepared for cell analysis. Single intestinal cells were prepared as previously described (60). Cells were stained with Cell Viability Dye (eBioscience), and cell surface staining of murine CD45 (clone 30-F11, eBioscience) and human CD4, CD146, and CCR5 or intracellular staining of IL-17 and IFN-γ after PMA and ionomycin stimulation were performed as described above. At day 45 after transplantation, 37.9% ± 2.9% and 11.0% ± 3.7% (n = 10) human $CD4^+$ T cells in the intestines expressed CD146 in the control shRNA group and CD146 shRNA group, respectively.

Statistics. Differences in characteristics between patient groups were assessed using Kruskal-Wallis tests for continuous values and χ^2 tests of association for categorical values. Frequencies of T cell subsets were compared using 2-tailed Student's t tests. Receiver operating characteristic (ROC) curves were generated, and the AUCs were estimated nonparametrically. The squared Pearson correlation coefficient was used for correlation analysis between markers, and the Spearman test was used for correlation between frequencies and absolute counts. Differences in immunohistochemical staining of GI biopsies were calculated using the 2-tailed Student's t test. Event-free survival was estimated using Kaplan-Meier analysis, and NRM and relapse mortality (RM) were modeled with cumulative incidence regression methods as described by Fine and Gray (77). In vitro data were compared using 2-tailed Student's t tests or paired t tests for in vitro transmigration assays performed with the same donor or 1-way ANOVA. $P < 0.05$ was considered to be statistically significant.

Study approval. The human studies were performed under protocols approved by the University of Michigan IRB (2001-0234, study HUM00036058) and after proof of informed consent. All animal experiments and euthanasia protocols were approved by the Indiana University School of Medicine institutional animal care committee (IACUC, protocol 10488).

Author contributions

WL and LL designed, performed, and analyzed in vitro and in vivo research and wrote the paper. AG designed and performed experiments, analyzed patient data, and wrote the paper. JZ and AR performed NanoString and in vivo research and wrote the paper. QZ and SH designed and performed experiments and analyzed proteomics data. SWC analyzed clinical patient data. PZ statistically analyzed patient data. JKG performed pathologic analysis of patient biopsies. CL performed pathologic analysis of samples from the in vivo experimental models. EV, SLK, and HH provided essential materials and help with the lentiviral work. DJ and HWC provided CD146 KO mice. RF and BRB performed and analyzed in vivo research. SP conceived the project; designed, performed, and analyzed the research; and wrote the paper.

Acknowledgments

This work was supported by the NIH (RC1 HL101102, R01 CA168814, P01 CA142106, P01 AI056299), the Amy Strelzer Manasevit Research Program, the Leukemia & Lymphoma Society Scholar Award, and the Lilly Physician Scientist Initiative Award. The authors thank Chrystal Paulos for suggestions on ICOS antibody–coated bead protocols. The authors thank the operators of the Indiana University Melvin and Bren Simon Cancer Center Flow Cytometry Resource Facility for their outstanding technical help. The Flow Cytometry Resource Facility is partially funded by the National Cancer Institute (P30 CA082709). We also acknowledge the help and support of the In Vivo Therapeutics Core of the Indiana University Melvin and Bren Simon Cancer Center (partially funded by the National Cancer Institute [P30 CA082709] and National Institute of Diabetes and Digestive and Kidney Diseases [P01 DK090948]).

Address correspondence to: Sophie Paczesny, Indiana University School of Medicine, 1044 W. Walnut Street, Room R4-425, Indianapolis, Indiana 46202, USA. Phone: 317.278.5487; E-mail: sophpacz@iu.edu.

1. Horowitz MM, et al. Graft-versus-leukemia reactions after bone marrow transplantation. *Blood*. 1990;75(3):555–562.
2. Warren EH, Deeg HJ. Dissecting graft-versus-leukemia from graft-versus-host-disease using novel strategies. *Tissue Antigens*. 2013;81(4):183–193.
3. Blazar BR, Murphy WJ, Abedi M. Advances in graft-versus-host disease biology and therapy. *Nat Rev Immunol*. 2012;12(6):443–458.
4. Deeg HJ, Antin JH. The clinical spectrum of acute graft-versus-host disease. *Semin Hematol*. 2006;43(1):24–31.
5. Cutler C, Antin JH. Manifestation and treatment of acute graft-versus-host-disease. In: Appelbaum F, Forman SJ, Negrin RS, Blume KG, eds. *Thomas' Hematopoietic Cell Transplantation*. 4th ed. Hoboken, New Jersey, USA: Blackwell Publishing Ltd; 2009:1287–1303.

6. Martin PJ, et al. Increasingly frequent diagnosis of acute gastrointestinal graft-versus-host disease after allogeneic hematopoietic cell transplantation. *Biol Blood Marrow Transpl*. 2004;10(5):320–327.
7. MacMillan ML, et al. Response of 443 patients to steroids as primary therapy for acute graft-versus-host disease: comparison of grading systems. *Biol Blood Marrow Transplant*. 2002;8(7):387–394.
8. Paczesny S, et al. A biomarker panel for acute graft-versus-host disease. *Blood*. 2009;113(2):273–278.
9. Ferrara JL, et al. Regenerating islet-derived 3-α is a biomarker of gastrointestinal graft-versus-host disease. *Blood*. 2011;118(25):6702–6708.
10. Vander Lugt MT, et al. ST2 as a marker for risk of therapy-resistant graft-versus-host disease and death. *N Engl J Med*. 2013;369(6):529–539.
11. Hansen JA, et al. A novel soluble form of Tim-3 associated with severe graft-versus-host disease. *Biol Blood Marrow Transplant*. 2013;19(9):1323–1330.
12. McDonald GB, Tabellini L, Storer BE, Lawler RL, Martin PJ, Hansen JA. Plasma biomarkers of acute GVHD and nonrelapse mortality: predictive value of measurements before GVHD onset and treatment. *Blood*. 2015;126(1):113–120.
13. Levine JE, et al. A prognostic score for acute graft-versus-host disease based on biomarkers: a multicenter study. *Lancet Haematol*. 2015;2(1):e21–e29.
14. MacMillan ML, et al. A refined risk score for acute graft-versus-host disease that predicts response to initial therapy, survival, and transplant-related mortality. *Biol Blood Marrow Transplant*. 2015;21(4):761–767.
15. Lehmann JM, Riethmuller G, Johnson JP. MUC18, a marker of tumor progression in human melanoma, shows sequence similarity to the neural cell adhesion molecules of the immunoglobulin superfamily. *Proc Natl Acad Sci U S A*. 1989;86(24):9891–9895.
16. Lehmann JM, Holzmann B, Breitbart EW, Schmiegelow P, Riethmuller G, Johnson JP. Discrimination between benign and malignant cells of melanocytic lineage by two novel antigens, a glycoprotein with a molecular weight of 113,000 and a protein with a molecular weight of 76,000. *Cancer Res*. 1987;47(3):841–845.
17. Tsiolakidou G, Koutroubakis IE, Tzardi M, Kouroumalis EA. Increased expression of VEGF and CD146 in patients with inflammatory bowel disease. *Dig Liver Dis*. 2008;40(8):673–679.
18. Bardin N, et al. Increased expression of CD146, a new marker of the endothelial junction in active inflammatory bowel disease. *Inflamm Bowel Dis*. 2006;12(1):16–21.
19. Elshal MF, et al. A unique population of effector memory lymphocytes identified by CD146 having a distinct immunophenotypic and genomic profile. *BMC Immunol*. 2007;8:29.
20. Pickl WF, et al. MUC18/MCAM (CD146), an activation antigen of human T lymphocytes. *J Immunol*. 1997;158(5):2107–2115.
21. Elshal MF, Khan SS, Takahashi Y, Solomon MA, McCoy JP Jr. CD146 (Mel-CAM), an adhesion marker of endothelial cells, is a novel marker of lymphocyte subset activation in normal peripheral blood. *Blood*. 2005;106(8):2923–2924.
22. Larochelle C, et al. Melanoma cell adhesion molecule identifies encephalitogenic T lymphocytes and promotes their recruitment to the central nervous system. *Brain*. *2012;*135(pt 10):2906–2924.
23. Guezguez B, Vigneron P, Lamerant N, Kieda C, Jaffredo T, Dunon D. Dual role of melanoma cell adhesion molecule (MCAM)/CD146 in lymphocyte endothelium interaction: MCAM/CD146 promotes rolling via microvilli induction in lymphocyte and is an endothelial adhesion receptor. *J Immunol*. 2007;179(10):6673–6685.
24. Xing S, et al. Targeting endothelial CD146 attenuates colitis and prevents colitis-associated carcinogenesis. *Am J Pathol*. 2014;184(5):1604–1616.
25. Schulz-Knappe P, et al. HCC-1, a novel chemokine from human plasma. *J Exp Med*. 1996;183(1):295–299.
26. Blain KY, et al. Structural and functional characterization of CC chemokine CCL14. *Biochemistry*. 2007;46(35):10008–10015.
27. Kotarsky K, et al. A novel role for constitutively expressed epithelial-derived chemokines as antibacterial peptides in the intestinal mucosa. *Mucosal Immunol*. 2010;3(1):40–48.
28. Detheux M, et al. Natural proteolytic processing of hemofiltrate CC chemokine 1 generates a potent CC chemokine receptor (CCR)1 and CCR5 agonist with anti-HIV properties. *J Exp Med*. 2000;192(10):1501–1508.
29. Wysocki CA, et al. Differential roles for CCR5 expression on donor T cells during graft-versus-host disease based on pretransplant conditioning. *J Immunol*. 2004;173(2):845–854.
30. Murai M, et al. Peyer's patch is the essential site in initiating murine acute and lethal graft-versus-host reaction. *Nat Immunol*. 2003;4(2):154–160.
31. Palmer LA, et al. Chemokine receptor CCR5 mediates alloimmune responses in graft-versus-host disease. *Biol Blood Marrow Transplant*. 2010;16(3):311–319.
32. Reshef RLS, et al. Blockade of lymphocyte chemotaxis in visceral graft-versus-host disease. *N Engl J Med*. 2012;367(2):135–145.
33. Paczesny S, et al. Elafin is a biomarker of graft-versus-host disease of the skin. *Sci Transl Med*. 2010;2(13):13ra2.
34. Dagur PK, et al. MCAM-expressing CD4(+) T cells in peripheral blood secrete IL-17A and are significantly elevated in inflammatory autoimmune diseases. *J Autoimmun*. 2011;37(4):319–327.
35. Sallusto F, Lenig D, Forster R, Lipp M, Lanzavecchia A. Two subsets of memory T lymphocytes with distinct homing potentials and effector functions. *Nature*. 1999;401(6754):708–712.
36. Muranski P, et al. Th17 cells are long lived and retain a stem cell-like molecular signature. *Immunity*. 2011;35(6):972–985.
37. Wei S, Zhao E, Kryczek I, Zou W. Th17 cells have stem cell-like features and promote long-term immunity. *Oncoimmunology*. 2012;1(4):516–519.
38. Paulos CM, et al. The inducible costimulator (ICOS) is critical for the development of human T(H)17 cells. *Sci Transl Med*. 2010;2(55):55ra78.
39. Loetscher P, et al. CCR5 is characteristic of Th1 lymphocytes. *Nature*. 1998;391(6665):344–345.
40. Bossard C, et al. Plasmacytoid dendritic cells and Th17 immune response contribution in gastrointestinal acute graft-versus-host disease. *Leukemia*. 2012;26(7):1471–1474.
41. Annunziato F, et al. Phenotypic and functional features of human Th17 cells. *J Exp Med*. 2007;204(8):1849–1861.
42. Awasthi A, et al. Cutting edge: IL-23 receptor gfp reporter mice reveal distinct populations of IL-17-producing cells. *J Immunol*. 2009;182(10):5904–5908.
43. Das R, et al. Blockade of interleukin-23 signaling results in targeted protection of the colon and allows for separation of graft-

versus-host and graft-versus-leukemia responses. *Blood*. 2010;115(25):5249–5258.
44. Lee Y, et al. Induction and molecular signature of pathogenic TH17 cells. *Nat Immunol*. 2012;13(10):991–999.
45. Kryczek I, et al. Human TH17 cells are long-lived effector memory cells. *Sci Transl Med*. 2011;3(104):104ra0.
46. Betts BC, et al. CD4+ T cell STAT3 phosphorylation precedes acute GVHD, and subsequent Th17 tissue invasion correlates with GVHD severity and therapeutic response. *J Leukoc Biol*. 2015;97(4):807–819.
47. Fulton LM, et al. Attenuation of acute graft-versus-host disease in the absence of the transcription factor RORγt. *J Immunol*. 2012;189(4):1765–1772.
48. Yu Y, et al. Prevention of GVHD while sparing GVL effect by targeting Th1 and Th17 transcription factor T-bet and RORγt in mice. *Blood*. 2011;118(18):5011–5020.
49. Despoix N, et al. Mouse CD146/MCAM is a marker of natural killer cell maturation. *Eur J Immunol*. 2008;38(10):2855–2864.
50. Edinger M, et al. CD4+CD25+ regulatory T cells preserve graft-versus-tumor activity while inhibiting graft-versus-host disease after bone marrow transplantation. *Nat Med*. 2003;9(9):1144–1150.
51. Magenau JM, et al. Frequency of CD4(+)CD25(hi)FOXP3(+) regulatory T cells has diagnostic and prognostic value as a biomarker for acute graft-versus-host-disease. *Biol Blood Marrow Transplant*. 2010;16(7):907–914.
52. Miura Y, et al. Association of Foxp3 regulatory gene expression with graft-versus-host disease. *Blood*. 2004;104(7):2187–2193.
53. Rezvani K, et al. High donor FOXP3-positive regulatory T-cell (Treg) content is associated with a low risk of GVHD following HLA-matched allogeneic SCT. *Blood*. 2006;108(4):1291–1297.
54. Duan H, et al. Targeting endothelial CD146 attenuates neuroinflammation by limiting lymphocyte extravasation to the CNS. *Sci Rep*. 2013;3:1687.
55. Flanagan K, et al. Laminin-411 is a vascular ligand for MCAM and facilitates TH17 cell entry into the CNS. *PLoS One*. 2012;7(7):e40443.
56. Ukena SN, et al. Human regulatory T cells in allogeneic stem cell transplantation. *Blood*. 2011;118(13):e82–e92.
57. Golovina TN, et al. CD28 costimulation is essential for human T regulatory expansion and function. *J Immunol*. 2008;181(4):2855–2868.
58. Weaver CT, Harrington LE, Mangan PR, Gavrieli M, Murphy KM. Th17: an effector CD4 T cell lineage with regulatory T cell ties. *Immunity*. 2006;24(6):677–688.
59. Nelson MH, et al. The inducible costimulator augments Tc17 cell responses to self and tumor tissue. *J Immunol*. 2015;194(4):1737–1747.
60. Zhang J, et al. ST2 blockade reduces sST2-producing T cells while maintaining protective mST2-expressing T cells during graft-versus-host disease. *Sci Transl Med*. 2015;7(308):308ra160.
61. Reichenbach DK, et al. The IL-33/ST2 axis augments effector T-cell responses during acute GVHD. *Blood*. 2015;125(20):3183–3192.
62. Gartlan KH, et al. Tc17 cells are a proinflammatory, plastic lineage of pathogenic CD8+ T cells that induce GVHD without antileukemic effects. *Blood*. 2015;126(13):1609–1620.
63. Serody JS, Hill GR. The IL-17 differentiation pathway and its role in transplant outcome. *Biol Blood Marrow Transplant*. 2012;18(1 suppl):S56–S61.
64. Schneider-Hohendorf T, et al. VLA-4 blockade promotes differential routes into human CNS involving PSGL-1 rolling of T cells and MCAM-adhesion of TH17 cells. *J Exp Med*. 2014;211(9):1833–1846.
65. van der Waart AB, van der Velden WJ, Blijlevens NM, Dolstra H. Targeting the IL17 pathway for the prevention of graft-versus-host disease. *Biol Blood Marrow Transplant*. 2014;20(6):752–759.
66. Taylor PA, et al. Targeting of inducible costimulator (ICOS) expressed on alloreactive T cells down-regulates graft-versus-host disease (GVHD) and facilitates engraftment of allogeneic bone marrow (BM). *Blood*. 2005;105(8):3372–3380.
67. Tajima N, et al. JTA-009, a fully human antibody against human AILIM/ICOS, ameliorates graft-vs-host reaction in SCID mice grafted with human PBMCs. *Exp Hematol*. 2008;36(11):1514–1523.
68. Faget J, et al. ICOS-ligand expression on plasmacytoid dendritic cells supports breast cancer progression by promoting the accumulation of immunosuppressive CD4+ T cells. *Cancer Res*. 2012;72(23):6130–6141.
69. Hanauer DA, Mei Q, Law J, Khanna R, Zheng K. Supporting information retrieval from electronic health records: A report of University of Michigan's nine-year experience in developing and using the Electronic Medical Record Search Engine (EMERSE). *J Biomed Inform*. 2015;55:290–300.
70. Lerner KG, Kao GF, Storb R, Buckner CD, Clift RA, Thomas ED. Histopathology of graft-vs.-host reaction (GvHR) in human recipients of marrow from HL-A-matched sibling donors. *Transplant Proc*. 1974;6(4):367–371.
71. Wiek C, et al. Identification of amino acid determinants in CYP4B1 for optimal catalytic processing of 4-ipomeanol. *Biochem J*. 2015;465(1):103–114.
72. Hanenberg H, Xiao XL, Dilloo D, Hashino K, Kato I, Williams DA. Colocalization of retrovirus and target cells on specific fibronectin fragments increases genetic transduction of mammalian cells. *Nat Med*. 1996;2(8):876–882.
73. Wu Q, et al. A novel function of MUC18: amplification of lung inflammation during bacterial infection. *Am J Pathol*. 2013;182(3):819–827.
74. Tawara I, et al. Interleukin-6 modulates graft-versus-host responses after experimental allogeneic bone marrow transplantation. *Clin Cancer Res*. 2011;17(1):77–88.
75. Reddy P, et al. Histone deacetylase inhibition modulates indoleamine 2,3-dioxygenase-dependent DC functions and regulates experimental graft-versus-host disease in mice. *J Clin Invest*. 2008;118(7):2562–2573.
76. Cooke KR, et al. An experimental model of idiopathic pneumonia syndrome after bone marrow transplantation: I. The roles of minor H antigens and endotoxin. *Blood*. 1996;88(8):3230–3239.
77. Fine JP, Gray RJ. A proportional hazards model for the subdistribution of a competing risk. *J Am Stat Assoc*. 1999;94:496–509.